Presynaptic Ultrastructural Plasticity Along CA3→CA1 Axons During Long-Term Potentiation in Mature Hippocampus

Jennifer N. Bourne,[1,3] Michael A. Chirillo,[1,2] and Kristen M. Harris[1]*

[1]Center for Learning and Memory, Section of Neurobiology, Institute for Neuroscience, University of Texas, Austin, Texas 78712
[2]University of Texas Medical School, Houston, Texas 77030
[3]Department of Physiology and Biophysics, University of Colorado, Anschutz Medical Campus, Aurora, CO 80045

ABSTRACT

In area CA1 of the mature hippocampus, synaptogenesis occurs within 30 minutes after the induction of long-term potentiation (LTP); however, by 2 hours many small dendritic spines are lost, and those remaining have larger synapses. Little is known, however, about associated changes in presynaptic vesicles and axonal boutons. Axons in CA1 *stratum radiatum* were evaluated with 3D reconstructions from serial section electron microscopy at 30 minutes and 2 hours after induction of LTP by theta-burst stimulation (TBS). The frequency of axonal boutons with a single postsynaptic partner was decreased by 33% at 2 hours, corresponding perfectly to the 33% loss specifically of small dendritic spines (head diameters <0.45 μm). Docked vesicles were reduced at 30 minutes and then returned to control levels by 2 hours following induction of LTP. By 2 hours there were fewer small synaptic vesicles overall in the presynaptic vesicle pool. Clathrin-mediated endocytosis was used as a marker of local activity, and axonal boutons containing clathrin-coated pits showed a more pronounced decrease in presynaptic vesicles at both 30 minutes and 2 hours after induction of LTP relative to control values. Putative transport packets, identified as a cluster of less than 10 axonal vesicles occurring between synaptic boutons, were stable at 30 minutes but markedly reduced by 2 hours after the induction of LTP. APV blocked these effects, suggesting that the loss of axonal boutons and presynaptic vesicles was dependent on N-methyl-D-aspartic acid (NMDA) receptor activation during LTP. These findings show that specific presynaptic ultrastructural changes complement postsynaptic ultrastructural plasticity during LTP. J. Comp. Neurol. 521:3898–3912, 2013.

INDEXING TERMS: synaptic vesicles; axonal boutons; vesicle pools; docked vesicles; serial section electron microscopy; 3D reconstruction; hippocampal slice

The relative presynaptic and postsynaptic contributions to long-term potentiation (LTP) are a topic of considerable investigation (Lisman and Harris, 1993; Kerchner and Nicoll, 2008). Quantal analyses (Malgaroli and Tsien, 1992; Stevens and Wang, 1994; Bolshakov et al., 1997; Sokolov et al., 2002; Choi et al., 2003), optical imaging of vesicles labeled with FM dyes or fluorescently tagged proteins (Ryan et al., 1996; Zakharenko et al., 2001, 2003; Bayazitov et al., 2007; Ratnayaka et al., 2012), and optical imaging of calcium influx into postsynaptic spines following stimulation of paired neurons (Emptage et al., 2003; Ward et al., 2006; Enoki et al., 2009) all provide supportive evidence for a presynaptic role during LTP. In addition, new puncta can form during LTP along axons of cultured neurons (Bozdagi et al., 2000; Antonova et al., 2001, 2009), and vesicles can be added to existing boutons to form new release sites (Kim et al., 2003). However, it has also been demonstrated that strictly postsynaptic changes, such as the insertion of α-amino-3-hydroxy-5-methylisoxazole-4-propionic acid (AMPA) receptors at silent and active synapses and the

Grant sponsor: National Institutes of Health (NIH); Grant numbers: NS21184, MH095980, and NS074644 (to K.M.H.).

*CORRESPONDENCE TO: Kristen M. Harris, PhD, Center for Learning and Memory, 1 University Station C7000, University of Texas, Austin, TX 78712. E-mail: kmh2249@gmail.com

Received February 12, 2013; Revised April 30, 2013;
Accepted June 7, 2013.
DOI 10.1002/cne.23384
Published online June 20, 2013 in Wiley Online Library (wileyonlinelibrary.com)

outgrowth of new spines, can sustain LTP for up to 1 hour (Kauer et al., 1988; Muller and Lynch, 1988; Manabe and Nicoll, 1994; Kullman, 1994; Liao et al., 1995; Nicoll and Malenka, 1995; Isaac et al., 1995; Shi et al., 1999; Matsuzaki et al., 2004; Kerchner and Nicoll, 2008). Recent work has shown rapid movement of extrasynaptic vesicles between boutons located more than 20 μm apart over a period of minutes both in vivo (Herzog et al., 2011) and in vitro (Darcy et al., 2006; Westphal et al., 2008; Staras et al., 2010). However, it is not known whether this mobilization of vesicles between axonal boutons is involved in the synaptic plasticity associated with LTP. Hence, many questions remain regarding the coordination of presynaptic and postsynaptic plasticity during LTP, especially at longer times after induction and in the mature hippocampus.

In mature hippocampal area CA1, 30 minutes after the induction of LTP with theta-burst stimulation (TBS), there is local synaptogenesis as evidenced by an increase in nonsynaptic protrusions both from the shaft of the dendrite and the head and neck of other spines (Bourne and Harris, 2011). However, by 2 hours, 33% of small dendritic spines (head diameters <0.45 μm) are lost. This loss is coupled to a corresponding enlargement of synapses on the remaining dendritic spines, which scales perfectly such that the summed synaptic area per unit length of dendrite is the same at all times after the induction of LTP (Bourne and Harris, 2011). It is known from past in vivo studies that the number of presynaptic vesicles scales with the surface area of the postsynaptic density (Harris and Stevens, 1989; Lisman and Harris, 1993; Harris and Sultan, 1995; Schikorski and Stevens, 2001), thus one might expect the number of vesicles to increase with LTP. However, prior single-section electron microscopy (EM) analyses of hippocampal dentate gyrus and area CA1 suggested that presynaptic vesicles numbers are reduced shortly after induction of LTP (Fifkova and Van Harreveld, 1977; Applegate et al., 1987; Meshul and Hopkins, 1990). Numerous studies suggest that LTP has distinct underlying mechanisms at 30 minutes and 2 hours (Abraham and Williams, 2003; Raymond, 2007; Reymann and Frey, 2007). Hence, we wanted to learn whether changes in presynaptic structure accompany the postsynaptic changes in synapse number and size at these functionally distinct times following the induction of LTP. We demonstrate through 3D reconstructions from serial section EM robust changes in axons, presynaptic vesicles, and extrasynaptic vesicles that correspond to the postsynaptic ultrastructural plasticity previously demonstrated during LTP in the mature hippocampus.

MATERIALS AND METHODS

Preparation and recording from acute hippocampal slices

Hippocampal slices were prepared from seven young adult male Long Evans rats aged 56–65 days old (weighing 263–361 g). All procedures were approved by the University of Texas at Austin Institutional Animal Care and Use Committee and the Institutional Biosafety Committee and followed the National Institutes of Health guidelines for the humane care and use of laboratory animals. Animals were anesthetized with halothane and decapitated, and slices were prepared at room temperature (~25°C) using artificial cerebrospinal fluid (ACSF) containing (in mM): 116.4 NaCl, 5.4 KCl, 3.2 $CaCl_2$, 1.6 $MgSO_4$, 26.2 $NaHCO_3$, 1.0 NaH_2PO_4, and 10 D-glucose. Slices were transferred in less than 5 minutes to nets positioned over wells containing ACSF at the interface of humidified O_2 (95%) and CO_2 (5%); slices then were maintained at 32°C for at least 3 hours in these in vitro chambers prior to experimentation. For the APV experiments ($n = 2$ slices from 2 animals), 50 μM D-2-amino-5-phosphonopentanoic acid (Sigma-Aldrich, St. Louis, MO) in ACSF was transferred into the wells at the end of the 3-hour preincubation period and remained for the duration of the experiment. Two concentric bipolar electrodes (Fred Haer, Brunswick, ME) were located 300–400 μm on either side of a single extracellular recording electrode placed in the middle of *stratum radiatum* (glass micropipette filled with 120 mM NaCl) for a total separation of 600–800 μm (Fig. 1A). Extracellular field potentials were recorded using IGOR software, and stimulations were alternated between the electrodes once every 2 minutes at a 30-second interval between electrodes (Bourne and Harris, 2011). Prior work has shown that optimal synaptic ultrastructure, which is comparable to perfusion-fixed hippocampus in vivo, is preserved for many hours in vitro under these conditions of slice preparation and maintenance (Bourne et al., 2007).

LTP paradigm

To begin, a stimulus/response curve was acquired for both stimulating electrodes at the two sites in the middle of *s. radiatum* in each slice; then a stable baseline was established at ~50% maximal response for 30 minutes (one pulse every 2 minutes) (Fig. 1B–D). Theta burst stimulation (TBS: 8 trains of 10 bursts at 5 Hz of 4 pulses at 100 Hz delivered 30 seconds apart, requiring 3.5 minutes in total) was delivered to one stimulating electrode at the same stimulus intensity as baseline. The positions of the control and TBS electrodes were alternated between the CA3 and subicular

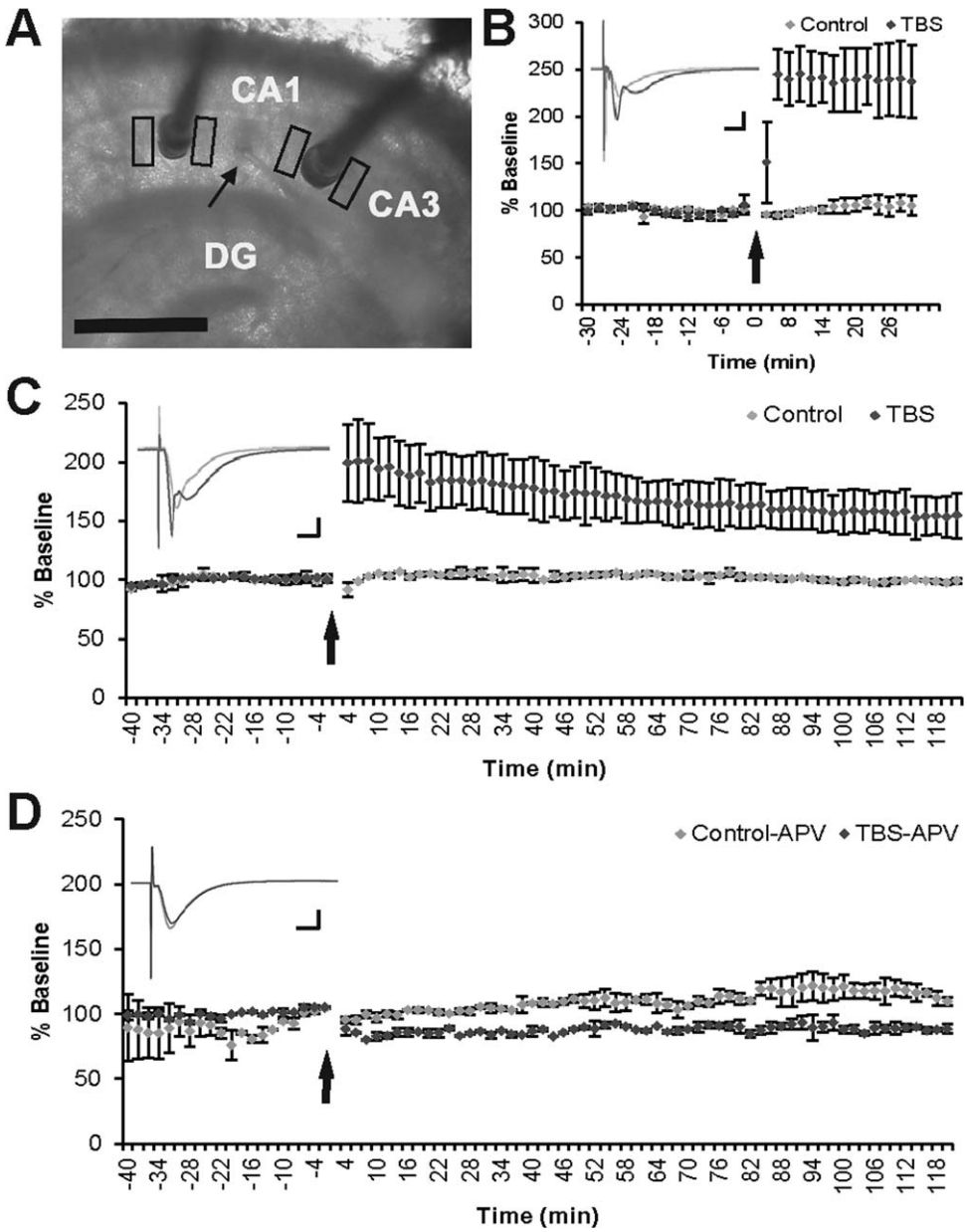

Figure 1. Site-specific LTP in hippocampal slices from adult rats is blocked by APV. **A:** A single recording electrode (arrow) was positioned in the middle of *s. radiatum* midway between two stimulating electrodes (dark posts) Tissue for analyses was collected immediately adjacent to the stimulating electrodes (black boxes). TBS was delivered to one of the stimulating electrodes at time 0 (arrow) to induce LTP (dark gray diamonds), and baseline stimulation was maintained at the other electrode (light gray diamonds). The responses were monitored for **(B)** 30 minutes (n = 3 slices from 3 animals), or **(C)** 2 hours (n = 2 slices from 2 animals) after the delivery of the first theta burst stimulation. **D:** TBS delivered in the presence of 50 μM APV did not induce LTP (n = 2 slices from 2 animals). Example waveforms for each time (insets in B–D) are an average across the entire pre-TBS (light gray) and post-TBS (dark gray) responses at the TBS site. Scale bars = 5mV/5ms (Adapted from Bourne and Harris, 2011). Scale bar = 500 μm in A.

sides of the recording electrode, counterbalancing across experiments. Responses from both stimulating electrodes were monitored (one pulse every 2 minutes) for 30 minutes or for 2 hours after the end of the first train of TBS for the LTP and APV experiments (Fig. 1B–D). The delivery of TBS resulted in robust potentiation relative to control (% baseline ± SD: 30 minutes LTP: 234 ± 22; 30 minutes Control: 103 ± 4; 2 hours LTP: 170 ± 32; 2 hours Control: 96 ± 5) that was blocked in the presence of 50 μM APV (Table 1) (% baseline ± SD: TBS-APV: 88 ± 6; Control-APV: 109 ± 11). The slices were then fixed by immersion in mixed aldehydes (6% glutaraldehyde and 2% paraformaldehyde in 100 mM cacodylate buffer with 2 mM $CaCl_2$ and 4 mM

TABLE 1.

Delivery of TBS in the Presence of 50 μM D-APV Had No Significant Effects on All But One of the Quantified Parameters (*)

Experimental condition	APV-Ctrl	APV-TBS	*P*-values
N (animals, axons, boutons)	2 animals, 20 axons, 62 boutons	2 animals, 20 axons, 53 boutons	
SSBs (#/μm^3)	2.04 ± 0.11	1.72 ± 0.13	0.20
MSBs (#/μm^3)	0.54 ± 0.08	0.2 ± 0.11	0.13
NSBs (#/μm^3)	0.58 ± 0.02	0.73 ± 0.13	0.36
Docked vesicles	3.71 ± 0.3	3.68 ± 0.4	0.95
Vesicle pool	311.39 ± 33.97	363.51 ± 41.7	0.24
Docked vesicles CCP-	3.79 ± 0.4	3.21 ± 0.4	0.31
Docked vesicles CCP+	3.57 ± 0.42	4.78 ± 0.91	0.01*
Vesicle Pool CCP-	266.33 ± 31.6	324.43 ± 40.7	0.30
Vesicle pool CCP+	406 ± 79.17	453.87 ± 100.03	0.10
% Transport packets/axon	21.64 ± 4.21	14.75 ± 4.01	0.24
Total vesicles α PSD area	$r = 0.61$, $P < 0.001$	$r = 0.84$, $P < 0.001$	
Docked vesicles α PSD area	$r = 0.74$, $P < 0.001$	$r = 0.79$, $P < 0.001$	

Results are shown as mean ± standard error, or as correlations (*r*) and significance of the correlation within condition.

$MgSO_4$) during 10 seconds of microwave irradiation to enhance diffusion of the fixative to the middle of the slice with a final temperature less than 35°C, and then post-fixed in the same fixative overnight at room temperature (Jensen and Harris, 1989). After fixation, slices were processed, ultrathin-sectioned, and imaged for serial section transmission electron microscopy as previously described (Bourne and Harris, 2011).

3D reconstructions and measurements

Serial sections were cut from a small trapezoid positioned in the middle of the region of optimal tissue preservation, ~100 μm from the slice air surface, and mounted on Pioloform-coated slot grids (Synaptek, Ted Pella, Redding, CA). Sections were counterstained with saturated ethanolic uranyl acetate followed by Reynolds lead citrate for 5 minutes each. Sections were imaged, blind as to condition, on a JEOL 1230 electron microscope with a Gatan digital camera at 5000× magnification.

The serial sections were aligned and axons were traced using the Reconstruct software (available for free download at http://synapses.clm.utexas.edu; Fiala, 2005). Section dimensions were calibrated using a diffraction grating replica (Ernest Fullam, Latham, NY) imaged with each series, and the cylindrical diameters method was used to compute section thickness by dividing the diameters of longitudinally sectioned mitochondria by the number of sections they spanned (Fiala and Harris, 2001a). The computed section thicknesses ranged from 38–60 nm and were not correlated with condition.

The area of a cross-sectioned synapse was calculated by measuring its length on each section and multiplying by section thickness and the number of sections traversed. Enclosed areas of en face and obliquely sectioned postsynaptic densities (PSDs) were measured on the section they appeared and added to the area computed for the cross-sectioned portions of that synapse. Vesicles were counted in presynaptic boutons; in addition, axons were traced across their lengths and vesicles were counted in at least two neighboring axonal boutons. (See figure legends for relevant N's.) Adobe Photoshop (San Jose, CA) was used to adjust the brightness and contrast of the electron micrographs in the figures.

Statistical analyses

Statistical analyses were done in the Statistica software package (StatSoft, Tulsa, OK). Two-way analysis of variance (ANOVA) was used to evaluate differences in axonal bouton frequencies at the TBS relative to control sites of stimulation for LTP and APV conditions, and at each timepoint with slice as the second variable (Figs. 3, 7). Changes in vesicle number per axonal bouton were analyzed using a nested hierarchical ANOVA with axon nested in condition and experiment (Figs. 4–6). For all analyses, data are plotted as means overlaid with individual data points. Then, to visualize the relative differences between LTP and control values, individual measurements were subtracted from the mean control value within each slice and plotted as the mean relative change (Δ mean, ± SEM) for each condition and timepoint.

RESULTS

TBS or control stimulation was delivered at electrodes positioned on either side of a recording electrode

positioned in the middle of *s. radiatum* of area CA1; the site of TBS nearer to CA3 or subiculum was counterbalanced across experiments such that each slice provided both conditions (Fig. 1A). Hippocampal slices were rapidly fixed at 30 minutes (Fig. 1B) or 2 hours after induction of LTP with TBS (Fig. 1C) (Bourne and Harris, 2011). To control for differential amounts of presynaptic activation, TBS and control stimulation were repeated in the presence of 50 μM APV, which blocked induction of LTP (Figure 1D, Table 1).

Serial section electron microscopy and 3D reconstruction were used to examine synaptic vesicles in 772 individual excitatory boutons. Complete axonal segments (192) were reconstructed for a subset of those boutons. Presumed glutamatergic excitatory axons were identified by the relatively round, clear vesicles contained in them and their association with dendritic spine synapses that had a thickened postsynaptic density (Fig. 2). Axonal boutons could be classified as single synaptic boutons (SSBs) if they had one postsynaptic partner (Fig. 2A), multisynaptic boutons (MSBs) if they had two or more postsynaptic partners (Fig. 2B), nonsynaptic boutons (NSBs) if they had more than 10 vesicles in a cluster but no postsynaptic partners (Fig. 2C). Representative 3D reconstructions illustrate the heterogeneity of axonal boutons along single axons (Fig. 2D–G). The frequency of mitochondria within axonal boutons was ~50% across all timepoints and conditions (30 minutes Control = 51% ± 4.8; 30 minutes LTP = 46% ± 8.6; 2 hours Control = 50% ± 6.4; 2 hours LTP = 53% ± 0.8; APV Control = 45% ± 1.2; APV-TBS = 56% ± 4.5).

Previously, we determined that small dendritic spines (with head diameters <0.45 μm) were decreased in number by 33% at 2 hours after the induction of LTP in these same slices (Bourne and Harris, 2011). Hence, we wanted to determine whether axonal boutons were also lost or if they simply became devoid of postsynaptic partners, so we performed an unbiased 3D brick analysis (Fiala and Harris, 2001b). A 3.5 × 3.5 μm sampling frame was positioned over the sample area on 50 serial sections, which then contained the largest axonal boutons (Fig. 3A). All boutons contained within the grid or touching the two inclusion lines (green) were counted. A total of 1,334 excitatory axonal boutons were followed through the image volumes (including the area surrounding the images), and the adjacent serial sections (up to 100), to identify them as SSB, MSB, or NSB. If the boutons contacted one of the two exclusion lines (red) of the grid, they were not included (Fig. 3B). This gave an unbiased estimate of number per volume of each type of bouton (Fiala and Harris, 2001b). The density of each bouton type was calculated by dividing the total number of boutons by the total brick volume.

At 2 hours, but not 30 minutes, after the induction of LTP, SSBs were selectively lost ($P < 0.05$), while there was no significant change in the frequency of MSBs or NSBs at either timepoint (Fig. 3C,D). Delivery of TBS in the presence of APV prevented this significant decrease in SSBs (APV Control: SSB = 2.04 ± 0.11; MSB = 0.54 ± 0.08; NSB = 0.58 ± 0.02; APV-TBS: SSB = 1.72 ± 0.13; MSB = 0.2 ± 0.11; NSB = 0.73 ± 0.13). These findings suggest that the SSBs were the original presynaptic partners of the lost small spines and that an N-methyl-D-aspartic acid (NMDA)-dependent process was involved in this presynaptic change.

Next, we investigated whether the vesicle composition of the axonal boutons was altered during LTP. Each bouton contains vesicles of varying release competence (Murthy et al., 1997; Dobrunz, 2002), and induction of plasticity can increase the fraction of vesicles available for release (Ratnayaka et al., 2012). As such, vesicles were classified as either docked, which are thought to be part of the readily releasable pool (Harris and Sultan, 1995; Schikorski and Stevens, 2001; Branco et al., 2010), or nondocked, which comprise the reserve vesicle pool (Fig. 4A,B). At 30 minutes after the induction of LTP, the average number of docked vesicles per bouton was decreased ($P < 0.01$; Fig. 4C,D). In contrast, the overall vesicle pool size did not differ significantly between conditions at 30 minutes (Fig. 4E,F). By 2 hours, the average number of docked vesicles was similar to control levels (Fig. 4C,D); however, the average size of the vesicle pool was significantly decreased ($P < 0.001$; Fig. 4E,F). Delivering TBS in the presence of APV did not result in this long-lasting reduction in the number of docked or nondocked vesicles relative to control stimulation (APV-Control: Docked = 3.71 ± 0.3, Nondocked = 311.39 ± 33.97; APV-TBS: Docked = 3.68 ± 0.4, Nondocked = 363.51 ± 41.7). These findings suggest that the additional action potentials delivered during TBS were not sufficient to alter the vesicular composition of boutons and that the decrease in vesicles with LTP involved NMDA-receptor activation.

Synaptic vesicles in axonal boutons are recycled via endocytosis in order to sustain release (Murthy and De, 2003; Ryan, 2006; Haucke et al., 2011; Lou et al., 2012). Such a tight coupling between release and endocytosis suggests that anatomical evidence of endocytosis could serve to mark which boutons were undergoing presynaptic activity at the time of fixation. To investigate whether the change in number of docked and nondocked vesicles might be related to recycling, we focused on boutons that showed anatomical evidence of recycling via clathrin-coated pits (CCPs), an early stage of endocytosis. During control stimulation alone,

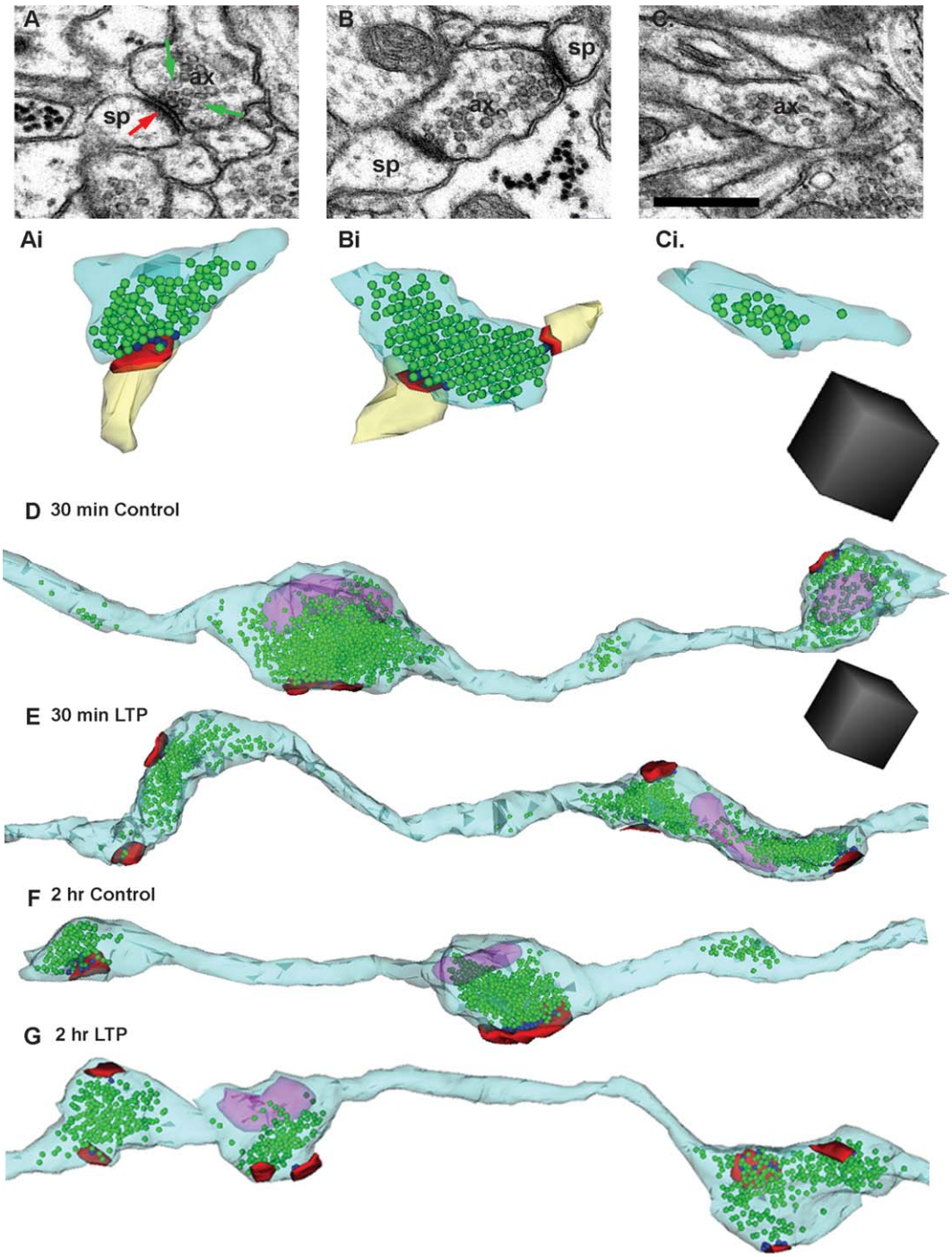

Figure 2. Heterogeneity of individual axonal boutons and axonal segments in area CA1 of the mature hippocampus. **A:** An EM and reconstruction of a single synaptic bouton (ax) filled with vesicles (green arrows) synapsing with the PSD (red arrow) on a dendritic spine (sp). **B:** An EM and reconstruction of a multisynaptic bouton (MSB) and both postsynaptic spine partners. **C:** An EM and reconstruction of a nonsynaptic bouton (NSB). **D–G:** 3D reconstructions of axons from each condition. Axon = light blue, nondocked vesicles = green, docked vesicles = blue, mitochondria = purple, PSD = red. Scale cube = 0.125 μm^3. Scale bar = 0.5 μm in C. [Color figure can be viewed in the online issue, which is available at wileyonlinelibrary.com.]

clathrin-coated pits (CCPs; Figs. 5A, 6A,C) were observed in 17% of boutons (Fig. 5B), and boutons with a CCP had more docked vesicles (Fig. 5C) and larger vesicle pools (Fig. 5D) than boutons without a CCP.

CCPs were also observed in some presynaptic boutons during LTP (Fig. 6B,D). The decrease in docked vesicles only reached statistical significance at 30 minutes in boutons without a CCP ($P < 0.01$; Fig. 6E,F).

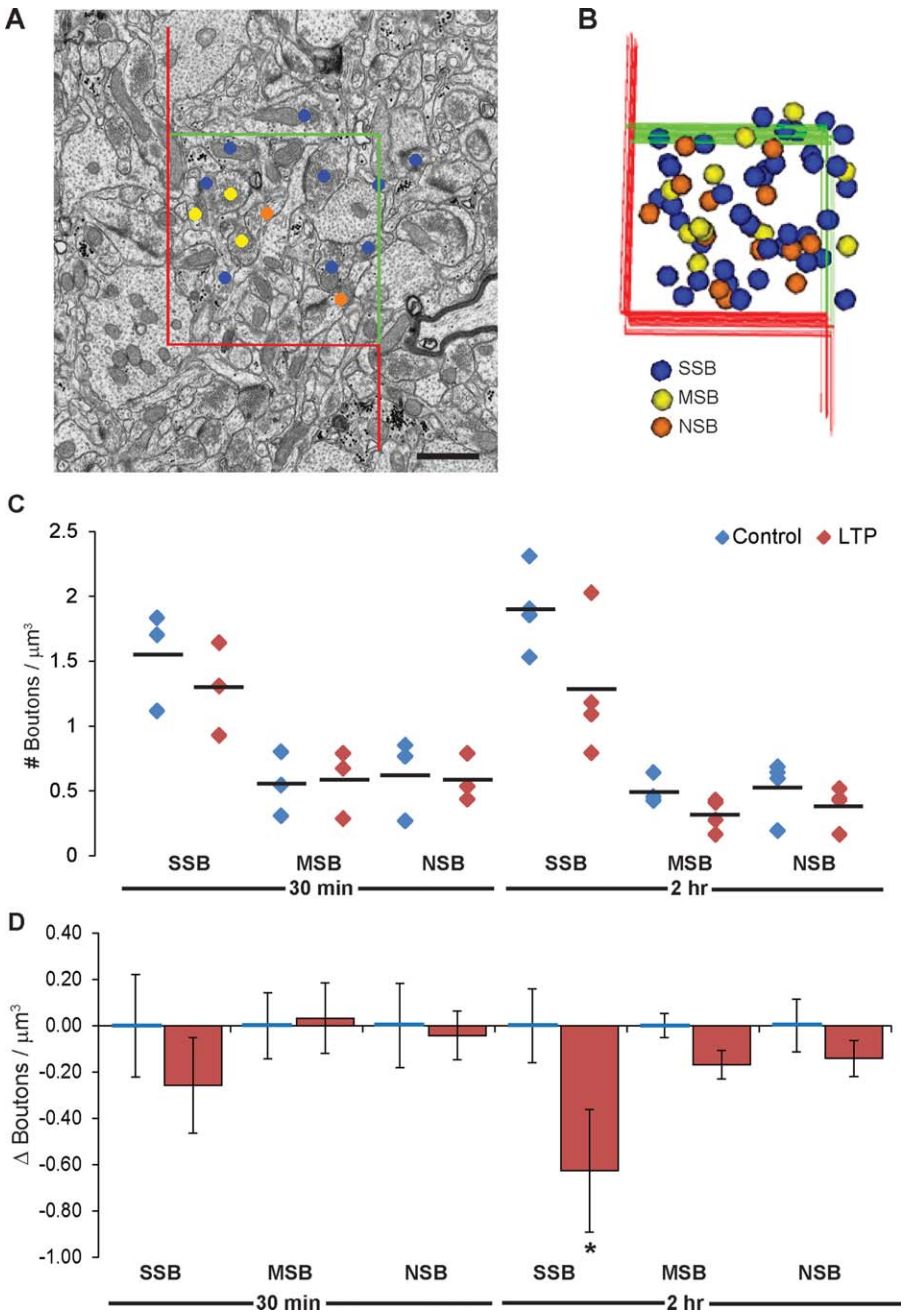

Figure 3. Single synaptic boutons are reduced at 2 hours after LTP induction. **A:** A sampling grid overlaid on an EM. Boutons within the grid or touching the green lines were included in the brick analysis, while boutons touching the red lines were excluded. **B:** Example of a brick in 3D with stamped boutons reconstructed as spheres. **C:** The average frequency of SSBs, MSBs, and NSBs for each condition. The distribution of the data is indicated by the diamonds and the means are represented by the superimposed black lines. 30 minutes data: $n = 3$ bricks each for Control and LTP; 2 hours data $n = 4$ bricks each for Control and LTP. **D:** Brick analyses of the neuropil volume revealed a loss of SSBs 2 hours after induction of LTP ($P < 0.05$) and no significant change in MSBs or NSBs (mean $\Delta \pm$ SEM). There was no significant change in the frequency of any boutons at 30 minutes after LTP induction. Scale bar = 1 µm in A. [Color figure can be viewed in the online issue, which is available at wileyonlinelibrary.com.]

The number of vesicles in the vesicle pool was significantly reduced at both 30 minutes and 2 hours during LTP for axonal boutons with a CCP ($P < 0.05$); by 2 hours, the vesicle pools were also smaller in boutons without a CCP ($P < 0.01$; Fig. 6G,H). There were no significant differences in the number of docked or nondocked vesicles when TBS was delivered in the presence of APV, regardless of the presence or absence of a CCP (APV-Control: Docked: +CCP = 3.57 ± 0.42, −CCP = 3.79 ± 0.4, Nondocked: +CCP =

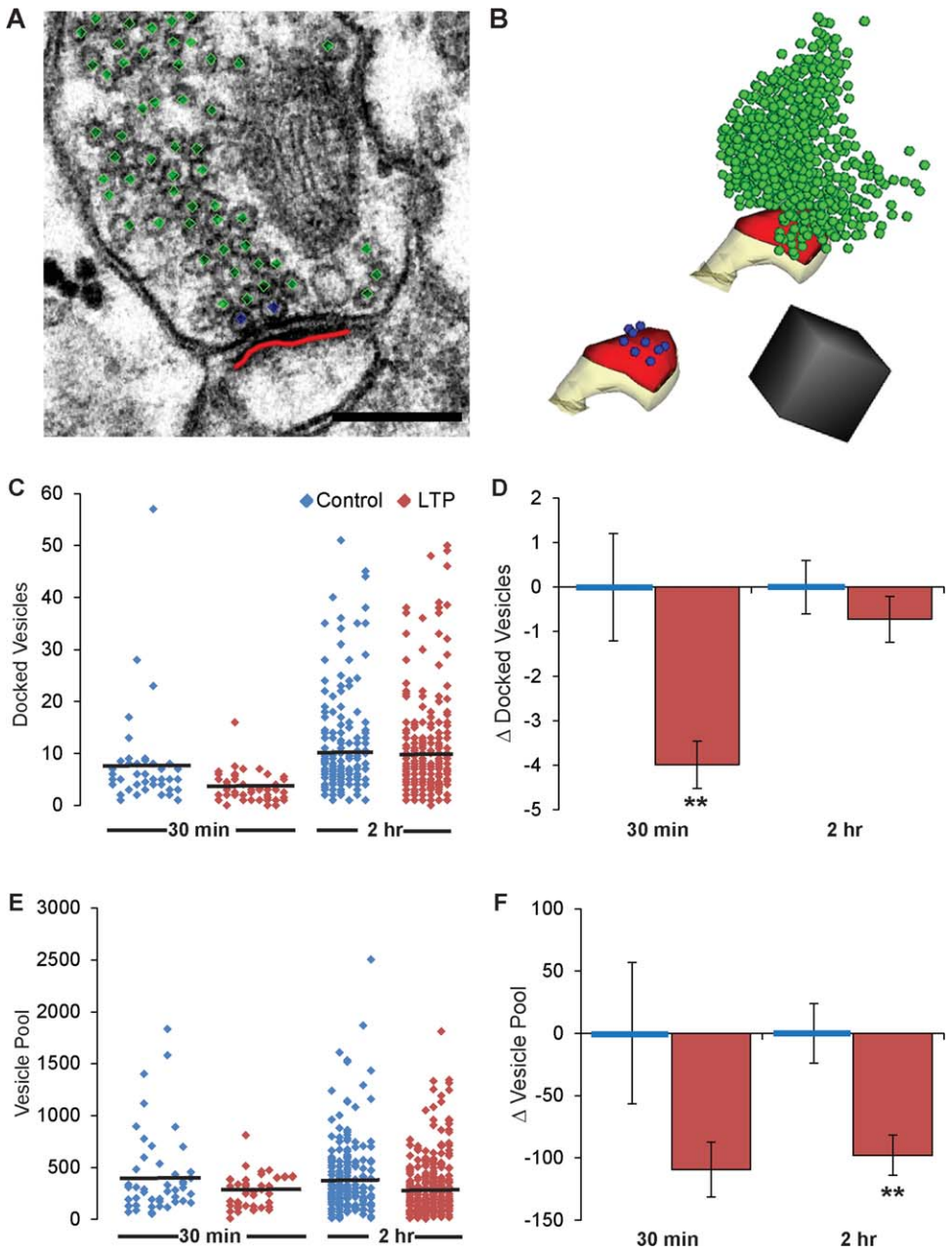

Figure 4. Decrease in docked vesicles at 30 minutes after LTP followed by reduction in vesicle pool by 2 hours. **(A)** EM and **(B)** 3D reconstruction of a dendritic spine (sp) and presynaptic bouton (ax) with the docked vesicles stamped in blue, the vesicle pool stamped in green, and PSD outlined in red. **C:** A graph of the average number of docked vesicles for each condition (black lines) with the distribution of the data indicated by the diamonds. **D:** The number of docked vesicles per presynaptic bouton decreased at 30 minutes after induction of LTP ($P < 0.01$, mean $\Delta \pm$ SEM). **E:** Graph representing the average number of nondocked vesicles (black lines) for each condition with the distribution of the data indicated by the diamonds. **F:** By 2 hours after LTP, the vesicle pool was significantly smaller ($P < 0.01$, mean $\Delta \pm$ SEM). 30 minutes Control: $n = 49$ boutons; 30 minutes LTP: $n = 59$ boutons; 2 hours Control: $n = 237$ boutons; 2 hours LTP: $n = 312$ boutons. Scale cube = 0.0156 μm^3. Scale bar = 0.25 μm in A. [Color figure can be viewed in the online issue, which is available at wileyonlinelibrary.com.]

406 ± 79.17, −CCP = 266.33 ± 31.6; APV-TBS: Docked, +CCP = 4.78 ± 0.91, −CCP = 3.21 ± 0.4, Nondocked, +CCP = 453.87 ± 100.03, −CCP = 324.43 ± 40.7). Thus, while boutons with evidence of recycling had a more pronounced reduction in their vesicle pool at 30 minutes and 2 hours after the induction of LTP, the longer lasting decrease was also observed in boutons without a CCP.

Vesicles are not restricted to presynaptic axonal boutons. Small "transport packets" of vesicles trafficking

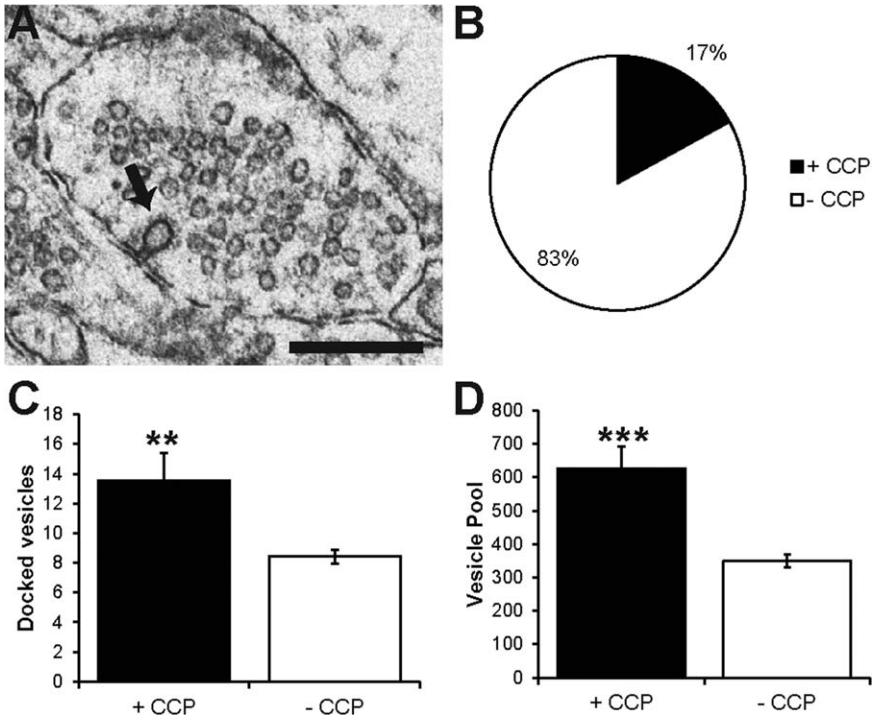

Figure 5. CCPs occur in presynaptic boutons with more docked vesicles and larger vesicle pools under control conditions. **A:** An EM of a control bouton with a CCP. **B:** The two sets of control data were combined from the 30 minutes and 2 hours experiments, and revealed overall that 17% of boutons contained a CCP ($n = 48$ boutons with a CCP and 238 boutons without a CCP). **C:** Boutons with a CCP had significantly more docked vesicles and **(D)** Larger vesicle pools than boutons lacking a CCP. Scale bar = 0.5 μm in A.

between boutons may also play an important role in synaptic plasticity (Ahmari et al., 2000; Ziv and Garner, 2004; Sabo et al., 2006) as key components of the vesicle "superpool" (Darcy et al., 2006; Westphal et al., 2008; Staras et al., 2010). Here we evaluated whether this interbouton transport might be altered during LTP by quantifying changes in the smallest NSBs, those containing 10 or fewer vesicles and classified as transport packets (Fig. 7A, arrow). Interestingly, 3% of these transport packets showed evidence of endocytosis (Fig. 7B,C), suggesting that some of the vesicles could be release competent during transit. At 30 minutes there was no significant difference in the number of transport packets between conditions; however, by 2 hours nearly all transport packets had been eliminated ($P < 0.01$; Fig. 7D,E). In the presence of APV, transport packet frequency did not change with control or TBS stimulation (APV-Control = 21.64 ± 4.21% per axon; APV-TBS = 14.75 ± 4.01% per axon). These data suggest a decrease in the interbouton trafficking of synaptic vesicles occurs by 2 hours after induction of LTP in the mature hippocampus.

DISCUSSION

Our findings show that significant presynaptic structural plasticity occurs during LTP induced by TBS. A decrease in docked synaptic vesicles at 30 minutes was followed by a more widespread reduction of vesicles in the pool, and a loss of presynaptic boutons by 2 hours. Small transport packets of vesicles were nearly eliminated by 2 hours after induction of LTP, suggesting that either they were incorporated into presynaptic boutons or their contents were released in transit. Blocking NMDA receptors during delivery of TBS prevented the loss of presynaptic boutons and the reduction of both docked and nondocked presynaptic vesicles, and retained transport of vesicles between boutons. Thus, LTP-specific changes occur in the vesicle composition of presynaptic boutons along CA3→CA1 axons of the mature hippocampus.

The loss of SSBs at 2 hours after induction of LTP is consistent with previous reports of increased turnover and dynamic remodeling of axonal boutons during synaptic plasticity in cultured neurons (Antonova et al., 2001; De Paola et al., 2003; Nikonenko et al., 2003). Boutons in the hippocampus and cortex remain dynamic into adulthood (De Paola et al., 2003; Umeda et al., 2005; Gogolla et al., 2007), and the presence of mobile transport packets or "orphan" boutons in cultured neurons suggests that release sites can form and disassemble quickly (Krueger et al., 2003). The

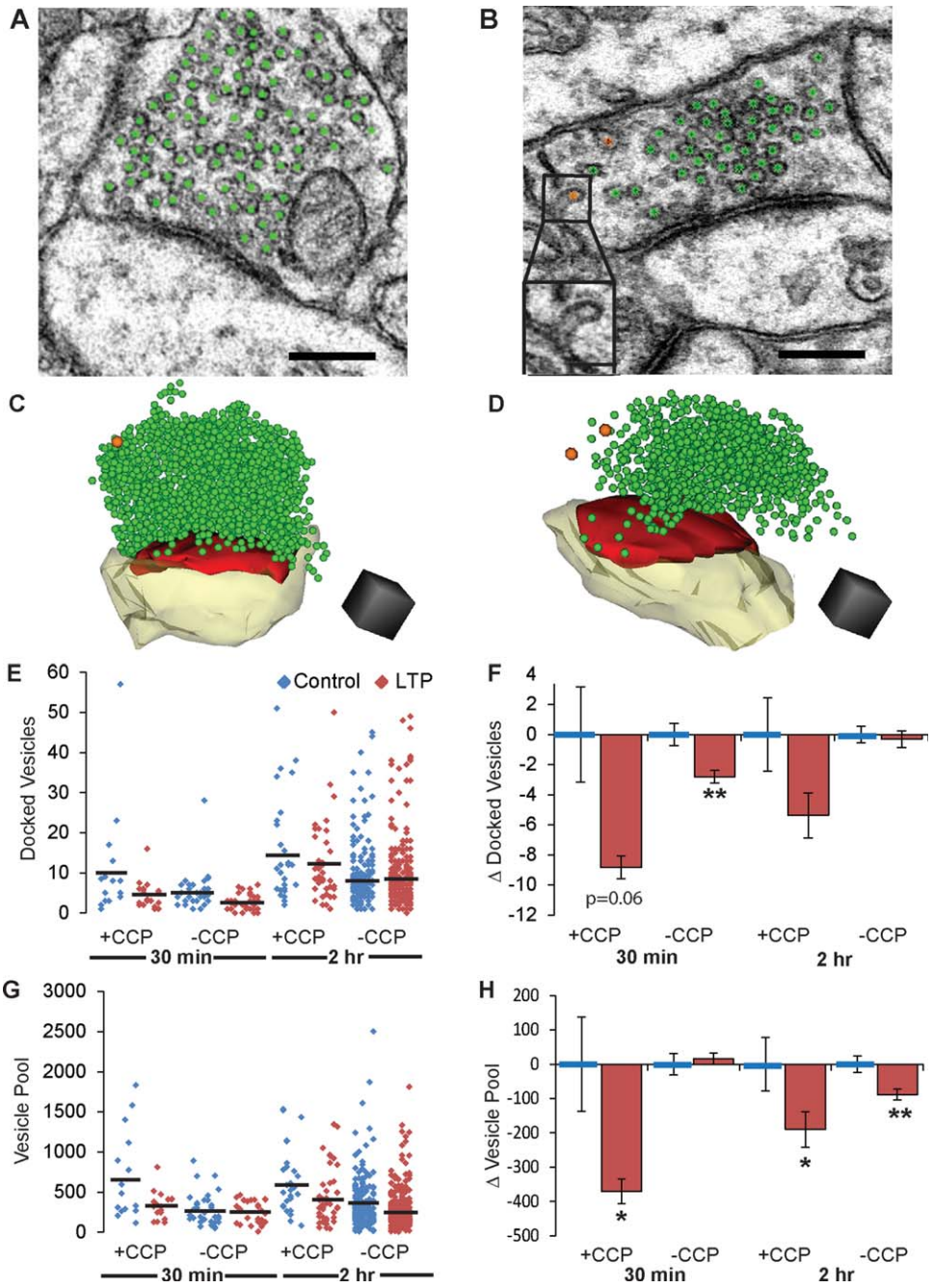

Figure 6. The number of vesicles was smaller in boutons with CCPs at both 30 minutes and 2 hours after LTP induction. **A:** An EM of a postsynaptic spine synapsing with a presynaptic axon from the 30 minutes Control condition. Nondocked vesicles of the pool are stamped in green. **B:** EM of a presynaptic bouton from the 2 hours LTP condition with two CCPs colored orange. **C:** 3D reconstruction of spine (yellow), PSD (red), nondocked vesicles (green), and a CCP (orange) from (A). **D:** Reconstruction from (B) with CCPs in orange. Scale cube = 0.0156 μm^3 for C,D. **E:** A graph of the average number of docked vesicles in axonal boutons with and without a CCP (black lines) across all conditions. Individual data points are represented by diamonds. **F:** At 30 minutes after LTP, the significant decrease in docked vesicles was observed in boutons without a CCP ($P < 0.01$, mean $\Delta \pm$ SEM). **G:** A graph of the average number (horizontal black lines) of nondocked vesicles in boutons with and without a CCP across all conditions. The distribution of the data is represented by the diamonds. **H:** A significant reduction (mean $\Delta \pm$ SEM) in vesicle pool size was observed in boutons with a CCP at 30 minutes ($P < 0.05$) and 2 hours ($P < 0.05$). 30 minutes Control: +CCP, $n = 16$ boutons, −CCP, $n = 33$ boutons; 30 minutes LTP: +CCP, $n = 20$ boutons, −CCP, $n = 39$ boutons; 2 hours Control: +CCP, $n = 32$ boutons; −CCP, $n = 205$ boutons; 2 hours LTP: +CCP, $n = 43$ boutons; −CCP, $n = 269$ boutons. Scale bars = 0.25 μm in A,B; inset, magnified CCP, 0.1 μm. [Color figure can be viewed in the online issue, which is available at wileyonlinelibrary.com.]

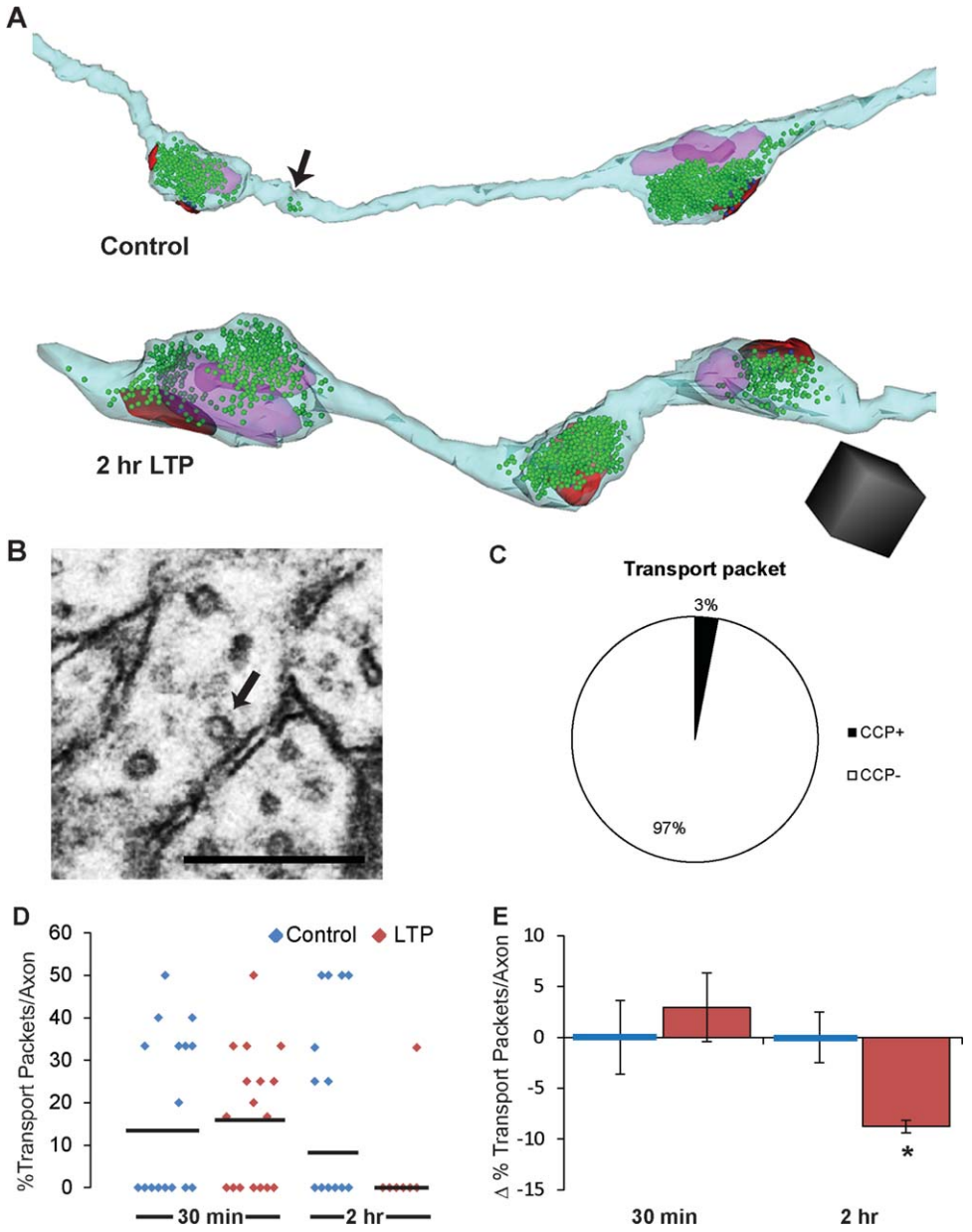

Figure 7. Transport packets are substantially reduced at 2 hours after induction of LTP. **A:** Reconstruction of axons from control and 2 hours LTP conditions. The control axonal bouton containing seven vesicles and no postsynaptic partners was considered to be a "transport packet" (black arrow). Axon = light blue, vesicles = green, mitochondria = purple, PSD = red. **B:** An EM of a transport packet with an omega figure (black arrow) indicating potential for release at a nonsynaptic site along an axon. **C:** A small fraction of transport packets contained a CCP ($n = 2$ transport packets with a CCP and $n = 71$ transport packets without a CCP). **D:** Average percentage of boutons along individual reconstructed axonal segments that were transport packets (black lines) with one data point per axon (diamonds); for each condition, most axons had no transport packets as illustrated by the concentration of data points at zero. **E:** The percentage of boutons along a reconstructed axonal segment that were transport packets (mean $\Delta \pm$ SEM) was significantly reduced at 2 hours after induction of LTP ($P < 0.05$), but not at 30 minutes. 30 minutes Control: $n = 21$ axons, 77 boutons; 30 minutes LTP: $n = 21$ axons, 78 boutons; 2 hours Control: $n = 52$ axons, 118 boutons; 2 hours LTP: $n = 58$ axons, 126 boutons. Scale cube = 0.125 μm^3. Scale bar = 0.25 μm in B. [Color figure can be viewed in the online issue, which is available at wileyonlinelibrary.com.]

decrease in SSBs at 2 hours after induction of LTP, without a corresponding increase in NSBs or MSBs, suggests that boutons were completely disassembled rather than converted to another type when small spines were eliminated. In fact, the 33% loss of SSBs corresponds perfectly with the 33% decrease in small thin spines discovered previously (Bourne and Harris, 2011), and thus the SSBs were likely the presynaptic

partners of the eliminated spines. These data also suggest that synapses are cohesive units and elimination of a postsynaptic spine during LTP triggers a corresponding disassembly of components in associated presynaptic axonal boutons. It further shows that axonal boutons along axons, i.e., en passant boutons, differ in their dynamics from terminal boutons, such as those found at the neuromuscular junction. While loss of a terminal bouton causes retraction of the axon (Bishop et al., 2004), loss of en passant SSBs is synapse specific and does not cause axonal retraction in mature hippocampus.

The number of vesicles docked at the active zone is thought to be indicative of release probability (Schikorski and Stevens, 2001; Harris and Sultan, 1995; Branco et al., 2010). Individual presynaptic boutons of CA3→CA1 axons can contain more than a thousand vesicles, yet less than 5% of all vesicles are docked and available for release (Harris and Sultan, 1995). In addition, the release probability of docked vesicles is heterogeneous across hippocampal boutons (Dobrunz and Stevens, 1997; Murthy et al., 1997), and minimal stimulation usually yields release of just one vesicle (Stevens and Wang, 1995; Hjelmstad et al., 1997; Hanse and Gustafsson, 2001). These observations raise the question: Why are there so many vesicles in the pool? One possibility is that multivesicular or enhanced exocytosis of the readily releasable pool during synaptic facilitation (Christie and Jahr, 2006) or LTP (Bolshakov et al., 1997; Zakharenko et al., 2001; Sokolov et al., 2002; Bayazitov et al., 2007; Enoki et al., 2009) results in vesicle reduction, which would be consistent with observations from cultured neurons where more vesicles were shown to be released and recycled during LTP (Ratnayaka et al., 2012). However, clathrin-mediated endocytosis can recycle fully collapsed vesicles within ~60 seconds (Rizzoli and Jahn, 2007), and the observation of CCPs suggests that exocytic/endocytic coupling was intact during LTP in the mature hippocampus. While an increase in full fusion events with LTP could saturate the endocytic machinery, a delay in recycling in a subset of boutons is unlikely, given that endocytosis kinetics appear to vary little from bouton to bouton (Armbruster and Ryan, 2011).

Although LTP may not alter the kinetics of the release and recycling of the readily releasable pool, it could have an impact on the reserve vesicle pool. Recently, it was discovered that the reserve pool (comprising ~80% of vesicles) was selectively involved in spontaneous release (Sara et al., 2005; Fredj and Burrone, 2009; Chung et al., 2010). This pool of vesicles has a slightly different complement of proteins including the v-SNARE VAMP7 rather than VAMP2 (Hua et al., 2011). VAMP7 preferentially binds to AP-3, an adaptor protein important for synaptic vesicle formation from endosomes (Faundez et al., 1998; Blumstein et al., 2001; Glyvuk et al., 2010) that is distinct from AP-2, which operates at the plasma membrane to recycle the readily-releasable pool (Di Paolo and De Camilli, 2006; Kim and Ryan, 2009). Vesicles expressing VAMP7 localize to the reserve pool and only undergo spontaneous release (Hua et al., 2011). Interestingly, the recycling of VAMP7 vesicles is much slower than the VAMP2 vesicles that comprise the readily releasable pool (Hua et al., 2011); hence, the reserve pool could be reduced if spontaneous release increased with LTP. Previous reports that mini-EPSP frequency increases with LTP (Bekkers and Stevens, 1990; Malgaroli and Tsien, 1992; Wiegert et al., 2009) support this idea that the reserve pool may be mobilized to enhance spontaneous release during synaptic plasticity.

Another possible explanation for the reduction in vesicles with LTP is that a nonrecyclable fraction of the vesicle pool contains elements to expand the active zone rather than neurotransmitter. Calcium channel accumulation at active zones is an essential regulator of neurotransmitter release (Yao et al., 2009; Graf et al., 2012; Holderith et al., 2012; Hoppa et al., 2012). The abundance of calcium channels at the synapse is determined by the size of the active zone (Holderith et al., 2012) and through interactions with proteins such as RIM, an organizer of the presynaptic release apparatus (Graf et al., 2012), and $\alpha 2\delta$, a subunit associated with voltage-gated calcium channels (VGCCs) (Hoppa et al., 2012). In *Drosophila*, a transmembrane calcium channel named Flower was identified in synaptic vesicles at the neuromuscular junction (Yao et al., 2009). Upon stimulation, fusion of the Flower-containing vesicles added calcium channels to the presynaptic membrane where they regulated resting intracellular calcium levels. While the majority of the Flower protein was removed with endocytosis, some of the protein remained in the presynaptic membrane. Thus, perhaps LTP recruits the exocytosis of vesicles that contain components of the active zone, such as calcium channels, to regulate dynamically the release properties of individual boutons. Future studies including immunolabeling of the vesicle pool will help elucidate the fraction of vesicles having functions beyond neurotransmitter release.

A superpool of vesicles has recently been discovered that can mobilize between neighboring boutons and participate in release (Darcy et al., 2006; Westphal et al., 2008; Staras et al., 2010). Recycling has been observed among vesicles in transport packets along axons of cultured neurons (Ratnayaka et al., 2011).

Here we discovered the first evidence for this extrasynaptic release and recycling in mature hippocampal (CA3→CA1) axons. In addition, the small transport packets were nearly eliminated by 2 hours after the induction of LTP, but not at 30 minutes. These data support findings from cultured neurons suggesting that the early stage of enhanced release with plasticity (<30 minutes) did not require extrasynaptic vesicle trafficking (Ratnayaka et al., 2012). However, by 2 hours after the induction of LTP, the widespread decrease in vesicle number appears to have recruited vesicles from transport packets to supplement their vesicle pools.

These results provide new evidence for coordinated pre- and postsynaptic structural scaling during LTP. We show that the elimination of small dendritic spines (Bourne and Harris, 2011) had a parallel loss of SSBs. There were fewer vesicles in the remaining boutons, suggesting elevated exocytosis, which may include increased spontaneous release of neurotransmitter and/or fusion of vesicles containing elements to expand the active zone. Elimination of transport packets further suggests that traveling vesicles of the "superpool" were either captured by the remaining boutons or released during transit. Thus, induction of LTP results in dramatic ultrastructural remodeling of axons in area CA1 of the mature hippocampus. Future research is needed to reveal variation in the content of the vesicle pools and whether they are replenished at later stages of LTP.

ACKNOWLEDGMENTS

JNB and KMH designed the experiments. JNB performed the experiments. JNB and MAC analyzed the images with confirmation from KMH on representative samples. JNB, MAC, and KMH analyzed the data and wrote the article. We thank Libby Perry and Robert Smith for technical support with EM processing and imaging.

LITERATURE CITED

Abraham WC, Williams JM. 2003. Properties and mechanisms of LTP maintenance. Neuroscientist 9:463–474.

Ahmari SE, Buchanan J, Smith SJ. 2000. Assembly of presynaptic active zones from cytoplasmic transport packets. Nat Neurosci 3:445–451.

Antonova I, Arancio O, Trillat AC, Wang HG, Zablow L, Udo H, Kandel ER, Hawkins RD. 2001. Rapid increase in clusters of presynaptic proteins at onset of long-lasting potentiation. Science 294:1547–1550.

Antonova I, Lu FM, Zablow L, Udo H, Hawkins RD. 2009. Rapid and long-lasting increase in sites for synapse assembly during late-phase potentiation in rat hippocampal neurons. PLoS One 4:e7690.

Applegate MD, Kerr DS, Landfield PW. 1987. Redistribution of synaptic vesicles during long-term potentiation in the hippocampus. Brain Res 401:401–406.

Armbruster M, Ryan TA. 2011. Synaptic vesicle retrieval time is a cell-wide rather than individual-synapse property. Nat Neurosci 14:824–826.

Bayazitov IT, Richardson RJ, Fricke RG, Zakharenko SS. 2007. Slow presynaptic and fast postsynaptic components of compound long-term potentiation. J Neurosci 27:11510–11521.

Bekkers JM, Stevens CF. 1990. Presynaptic mechanism for long-term potentiation in the hippocampus. Nature 346:724–729.

Bishop DL, Misgeld T, Walsh MK, Gan WB, Lichtman JW. 2004. Axon branch removal at developing synapses by axosome shedding. Neuron 44:651–661.

Blumstein J, Faundez V, Nakatsu F, Saito T, Ohno H, Kelly RB. 2001. The neuronal form of adaptor protein-3 is required for synaptic vesicle formation from endosomes. J Neurosci 21:8034–8042.

Bolshakov VY, Golan H, Kandel ER, Siegelbaum SA. 1997. Recruitment of new sites of synaptic transmission during the cAMP-dependent late phase of LTP at CA3-CA1 synapses in the hippocampus. Neuron 19:635–651.

Bourne JN, Harris KM. 2011. Coordination of size and number of excitatory and inhibitory synapses results in a balanced structural plasticity along mature hippocampal CA1 dendrites during LTP. Hippocampus 21:354–373.

Bourne JN, Kirov SA, Sorra KE, Harris KM. 2007. Warmer preparation of hippocampal slices prevents synapse proliferation that might obscure LTP-related structural plasticity. Neuropharmacology 52:55–59.

Bozdagi O, Shan W, Tanaka H, Benson DL, Huntley GW. 2000. Increasing numbers of synaptic puncta during late-phase LTP: N-cadherin is synthesized, recruited to synaptic sites, and required for potentiation. Neuron 28:245–259.

Branco T, Marra V, Staras K. 2010. Examining size-strength relationships at hippocampal synapses using an ultrastructural measurement of synaptic release probability. J Struct Biol 172:203–210.

Choi S, Klingauf J, Tsien RW. 2003. Fusion pore modulation as a presynaptic mechanism contributing to expression of long-term potentiation. Philos Trans R Soc Lond B Biol Sci 358:695–705.

Christie JM, Jahr CE. 2006. Multivesicular release at Schaffer collateral-CA1 hippocampal synapses. J Neurosci 26:210–216.

Chung C, Barylko B, Leitz J, Liu X, Kavalali ET. 2010. Acute dynamin inhibition dissects synaptic vesicle recycling pathways that drive spontaneous and evoked neurotransmission. J Neurosci 30:1363–1376.

Darcy KJ, Staras K, Collinson LM, Goda Y. 2006. Constitutive sharing of recycling synaptic vesicles between presynaptic boutons. Nat Neurosci 9:315–321.

De Paola V, Arber S, Caroni P. 2003. AMPA receptors regulate dynamic equilibrium of presynaptic terminals in mature hippocampal networks. Nat Neurosci 6:491–500.

Di Paolo G, De Camilli P. 2006. Phosphoinositides in cell regulation and membrane dynamics. Nature 443:651–657.

Dobrunz LE. 2002. Release probability is regulated by the size of the readily releasable vesicle pool at excitatory synapses in hippocampus. Int J Dev Neurosci 20:225–236.

Dobrunz LE, Stevens CF. 1997. Heterogeneity of release probability, facilitation, and depletion at central synapses. Neuron 18:995–1008.

Emptage NJ, Reid CA, Fine A, Bliss TV. 2003. Optical quantal analysis reveals a presynaptic component of LTP at hippocampal Schaffer-associational synapses. Neuron 38:797–804.

Enoki R, Hu YL, Hamilton D, Fine A. 2009. Expression of long-term plasticity at individual synapses in hippocampus is

graded, bidirectional, and mainly presynaptic: optical quantal analysis. Neuron 62:242–253.
Faundez V, Horng JT, Kelly RB. 1998. A function for the AP3 coat complex in synaptic vesicle formation from endosomes. Cell 93:423–432.
Fiala JC. 2005. Reconstruct: a free editor for serial section microscopy. J Microsc 218(Pt 1):52–61.
Fiala JC, Harris KM. 2001a. Cylindrical diameters method for calibrating section thickness in serial electron microscopy. J Microsc 202(Pt 3):468–472.
Fiala JC, Harris KM. 2001b. Extending unbiased stereology of brain ultrastructure to three-dimensional volumes. J Am Med Inform Assoc 8:1–16.
Fifkova E, Van Harreveld A. 1977. Long-lasting morphological changes in dendritic spines of dentate granular cells following stimulation of the entorhinal area. J Neurocytol 6: 211–230.
Fredj NB, Burrone J. 2009. A resting pool of vesicles is responsible for spontaneous vesicle fusion at the synapse. Nat Neurosci 12:751–758.
Glyvuk N, Tsytsyura Y, Geumann C, D'Hooge R, Huve J, Kratzke M, Baltes J, Boening D, Klingauf J, Schu P. 2010. AP-1/sigma1B-adaptin mediates endosomal synaptic vesicle recycling, learning and memory. EMBO J 29:1318–1330.
Gogolla N, Galimberti I, Caroni P. 2007. Structural plasticity of axon terminals in the adult. Curr Opin Neurobiol 17: 516–524.
Graf ER, Valakh V, Wright CM, Wu C, Liu Z, Zhang YQ, DiAntonio A. 2012. RIM promotes calcium channel accumulation at active zones of the Drosophila neuromuscular junction. J Neurosci 32:16586–16596.
Hanse E, Gustafsson B. 2001. Factors explaining heterogeneity in short-term synaptic dynamics of hippocampal glutamatergic synapses in the neonatal rat. J Physiol 537(Pt 1):141–149.
Harris KM, Stevens JK. 1989. Dendritic spines of CA1 pyramidal cells in the rat hippocampus: serial electron microscopy with reference to their biophysical characteristics. J Neurosci 9:2982–2997.
Harris KM, Sultan P. 1995. Variation in the number, location and size of synaptic vesicles provides an anatomical basis for the nonuniform probability of release at hippocampal CA1 synapses. Neuropharmacology 34:1387–1395.
Haucke V, Neher E, Sigrist SJ. 2011. Protein scaffolds in the coupling of synaptic exocytosis and endocytosis. Nat Rev Neurosci 12:127–138.
Herzog E, Nadrigny F, Silm K, Biesemann C, Helling I, Bersot T, Steffens H, Schwartzmann R, Nagerl UV, el MS, Rhee J, Kirchhoff F, Brose N. 2011. In vivo imaging of intersynaptic vesicle exchange using VGLUT1 Venus knock-in mice. J Neurosci 31:15544–15559.
Hjelmstad GO, Nicoll RA, Malenka RC. 1997. Synaptic refractory period provides a measure of probability of release in the hippocampus. Neuron 19:1309–1318.
Holderith N, Lorincz A, Katona G, Rozsa B, Kulik A, Watanabe M, Nusser Z. 2012. Release probability of hippocampal glutamatergic terminals scales with the size of the active zone. Nat Neurosci 15:988–997.
Hoppa MB, Lana B, Margas W, Dolphin AC, Ryan TA. 2012. alpha2delta expression sets presynaptic calcium channel abundance and release probability. Nature 486:122–125.
Hua Z, Leal-Ortiz S, Foss SM, Waites CL, Garner CC, Voglmaier SM, Edwards RH. 2011. v-SNARE composition distinguishes synaptic vesicle pools. Neuron 71:474–487.
Isaac JT, Nicoll RA, Malenka RC. 1995. Evidence for silent synapses: implications for the expression of LTP. Neuron 15:427–434.
Jensen FE, Harris KM. 1989. Preservation of neuronal ultrastructure in hippocampal slices using rapid microwave-enhanced fixation. J Neurosci Methods 29:217–230.
Kauer JA, Malenka RC, Nicoll RA. 1988. A persistent postsynaptic modification mediates long-term potentiation in the hippocampus. Neuron 1:911–917.
Kerchner GA, Nicoll RA. 2008. Silent synapses and the emergence of a postsynaptic mechanism for LTP. Nat Rev Neurosci 9:813–825.
Kim SH, Ryan TA. 2009. Synaptic vesicle recycling at CNS snapses without AP-2. J Neurosci 29:3865–3874.
Kim JH, Udo H, Li HL, Youn TY, Chen M, Kandel ER, Bailey CH. 2003. Presynaptic activation of silent synapses and growth of new synapses contribute to intermediate and long-term facilitation in Aplysia. Neuron 40:151–165.
Krueger SR, Kolar A, Fitzsimonds RM. 2003. The presynaptic release apparatus is functional in the absence of dendritic contact and highly mobile within isolated axons. Neuron 40:945–957.
Kullman DM. 1994. Amplitude fluctuations of dual-component EPSCs in hippocampal pyramidal cells: implications for long-term potentiation. Neuron 12:1111–1120.
Liao D, Hessler NA, Malinow R. 1995. Activation of postsynaptically silent synapses during pairing-induced LTP in CA1 region of hippocampal slice. Nature 375:400–404.
Lisman J, Harris KM. 1993. Quantal analysis and synaptic anatomy — integrating two views of hippocampal plasticity. Trends Neurosci 16:141–147.
Lou X, Fan F, Messa M, Raimondi A, Wu Y, Looger LL, Ferguson SM, De CP. 2012. Reduced release probability prevents vesicle depletion and transmission failure at dynamin mutant synapses. Proc Natl Acad Sci U S A 109:E515–E523.
Malgaroli A, Tsien RW. 1992. Glutamate-induced long-term potentiation of the frequency of miniature synaptic currents in cultured hippocampal neurons. Nature 357:134–139.
Manabe T, Nicoll RA. 1994. Long-term potentiation: Evidence against an increase in transmitter release probability in the CA1 region of the hippocampus. Science 265:1888–1891.
Matsuzaki M, Honkura N, Ellis-Davies GC, Kasai H. 2004. Structural basis of long-term potentiation in single dendritic spines. Nature 429:761–766.
Meshul CK, Hopkins WF. 1990. Presynaptic ultrastructural correlates of long-term potentiation CA1 subfield of the hippocampus. Brain Res 514:310–319.
Muller D, Lynch G. 1988. Long-term potentiation differentially affects two components of synaptic responses in hippocampus. Proc Natl Acad Sci U S A 85:9346–9350.
Murthy VN, De CP. 2003. Cell biology of the presynaptic terminal. Annu Rev Neurosci 26:701–728.
Murthy VN, Sejnowski TJ, Stevens CF. 1997. Heterogeneous release properties of visualized individual hippocampal synapses. Neuron 18:599–612.
Nicoll RA, Malenka RC. 1995. Contrasting properties of two forms of long-term potentiation in the hippocampus. Nature 377:115–118.
Nikonenko I, Jourdain P, Muller D. 2003. Presynaptic remodeling contributes to activity-dependent synaptogenesis. J Neurosci 23:8498–8505.
Ratnayaka A, Marra V, Branco T, Staras K. 2011. Extrasynaptic vesicle recycling in mature hippocampal neurons. Nat Commun 2:531.
Ratnayaka A, Marra V, Bush D, Burden JJ, Branco T, Staras K. 2012. Recruitment of resting vesicles into recycling pools supports NMDA-receptor dependent synaptic potentiation in cultured hippocampal neurons. J Physiol 590:1585–1597.

Raymond CR. 2007. LTP forms 1, 2 and 3: different mechanisms for the "long" in long-term potentiation. Trends Neurosci 30:167–175.

Reymann KG, Frey JU. 2007. The late maintenance of hippocampal LTP: requirements, phases, 'synaptic tagging', 'late-associativity' and implications. Neuropharmacology 52:24–40.

Rizzoli SO, Jahn R. 2007. Kiss-and-run, collapse and 'readily retrievable' vesicles. Traffic 8:1137–1144.

Ryan TA. 2006. A pre-synaptic to-do list for coupling exocytosis to endocytosis. Curr Opin Cell Biol 18:416–421.

Ryan TA, Ziv NE, Smith SJ. 1996. Potentiation of evoked vesicle turnover at individually resolved synaptic boutons. Neuron 17:125–134.

Sabo SL, Gomes RA, McAllister AK. 2006. Formation of presynaptic terminals at predefined sites along axons. J Neurosci 26:10813–10825.

Sara Y, Biederer T, Atasoy D, Chubykin A, Mozhayeva MG, Sudhof TC, Kavalali ET. 2005. Selective capability of SynCAM and neuroligin for functional synapse assembly. J Neurosci 25:260–270.

Schikorski T, Stevens CF. 2001. Morphological correlates of functionally defined synaptic vesicle populations. Nat Neurosci 4:391–395.

Shi SH, Hayashi Y, Petralia RS, Zaman SH, Wenthold RJ, Svoboda K, Malinow R. 1999. Rapid spine delivery and redistribution of AMPA receptors after synaptic NMDA receptor activation. Science 284:1811–1816.

Sokolov MV, Rossokhin AV, Astrelin AV, Frey JU, Voronin LL. 2002. Quantal analysis suggests strong involvement of presynaptic mechanisms during the initial 3 h maintenance of long-term potentiation in rat hippocampal CA1 area in vitro. Brain Res 957:61–75.

Staras K, Branco T, Burden JJ, Pozo K, Darcy K, Marra V, Ratnayaka A, Goda Y. 2010. A vesicle superpool spans multiple presynaptic terminals in hippocampal neurons. Neuron 66:37–44.

Stevens CF, Wang Y. 1994. Changes in reliability of synaptic function as a mechanism for plasticity. Nature 371:704–707.

Stevens CF, Wang Y. 1995. Facilitation and depression at single central synapses. Neuron 14:795–802.

Umeda T, Ebihara T, Okabe S. 2005. Simultaneous observation of stably associated presynaptic varicosities and postsynaptic spines: morphological alterations of CA3-CA1 synapses in hippocampal slice cultures. Mol Cell Neurosci 28:264–274.

Ward B, McGuinness L, Akerman CJ, Fine A, Bliss TV, Emptage NJ. 2006. State-dependent mechanisms of LTP expression revealed by optical quantal analysis. Neuron 52:649–661.

Westphal V, Rizzoli SO, Lauterbach MA, Kamin D, Jahn R, Hell SW. 2008. Video-rate far-field optical nanoscopy dissects synaptic vesicle movement. Science 320:246–249.

Wiegert JS, Hofmann F, Bading H, Bengtson CP. 2009. A transcription-dependent increase in miniature EPSC frequency accompanies late-phase plasticity in cultured hippocampal neurons. BMC Neurosci 10:124.

Yao CK, Lin YQ, Ly CV, Ohyama T, Haueter CM, Moiseenkova-Bell VY, Wensel TG, Bellen HJ. 2009. A synaptic vesicle-associated Ca2+ channel promotes endocytosis and couples exocytosis to endocytosis. Cell 138:947–960.

Zakharenko SS, Zablow L, Siegelbaum SA. 2001. Visualization of changes in presynaptic function during long-term synaptic plasticity. Nat Neurosci 4:711–717.

Zakharenko SS, Patterson SL, Dragatsis I, Zeitlin SO, Siegelbaum SA, Kandel ER, Morozov A. 2003. Presynaptic BDNF required for a presynaptic but not postsynaptic component of LTP at hippocampal CA1-CA3 synapses. Neuron 39:975–990.

Ziv NE, Garner CC. 2004. Cellular and molecular mechanisms of presynaptic assembly. Nat Rev Neurosci 5: 385–399.